Applied Mathematics and Optimization 4, 197–207 (1978)

Applied Mathematics and Optimization

Technical Note

Minimum Drag Surfaces*

William W. Hager[1] and Joel C. W. Rogers[2]

Communicated by S. K. Mitter

[1]Department of Mathematics, Carnegie-Mellon University, Pittsburgh, Pennsylvania, 15213.
[2]Applied Physics Laboratory, The Johns Hopkins University, Johns Hopkins Road, Laurel, Maryland 20810.

Abstract. We consider existence, uniqueness, and computation of minimum drag shapes for projectiles subjected to both Newtonian pressure drag and skin friction drag. Critical values of the drag coefficients are determined where the optimal shape changes from perfectly blunt to conical to partially blunt. The existence proof, based on duality theory, provides an efficient algorithm for computing the optimal shape.

I. Introduction

For projectiles traveling at zero angle of attack, we consider the existence, uniqueness, and computation of minimum drag shapes. We assume that the projectile is a solid of revolution (possibly nonslender) subjected to both Newtonian pressure drag and skin friction drag; our results differ from earlier work in the following aspects: Kennet [4] and Miele, Hull [5] only consider slender bodies while Eggers [1] ignores skin friction. Also our work is more mathematically oriented since we prove rigorously the existence and uniqueness of an optimal shape. The behavior of the optimal shape relative to the pressure and friction coefficients is studied, and we determine the critical values of the coefficients where the optimal shape changes from perfectly blunt to conical to partially blunt.

Our approach, fundamentally different from earlier work, is based on Lagrange duality theory for convex control problems developed by Hager and Mitter [2]. If the skin friction is sufficiently large, the optimum shape can be

*This work was supported in part by the Naval Surface Weapons Center, Silver Spring, Maryland, where both authors were employed during the Summer, 1976.

0095-4616/78/0004-0197 $02.20

determined analytically; however, for sea level conditions, the shape must be computed numerically. The usual algorithms for calculus of variation problems involve iterative procedures for either solving a related two-point boundary-value problem or evaluating the constant in the first integral equation. The algorithm presented below, on the other hand, is essentially direct—one differential equation is integrated to determine the value of a dual multiplier and a second equation is integrated to obtain the optimal shape.

II. Problem Statement and Principal Results

The following variational problem is considered:

$$\inf\left\{D(r)=2\int_0^{\ell}\left[c_1\frac{r(x)r'(x)^3}{1+r'(x)^2}+c_2 r(x)\sqrt{1+r'(x)^2}\right]dx\right\} \tag{2.1}$$

subject to $r(0)=0$, $r(\ell)=r_1$, $r'\geqslant 0$, r' essentially bounded, where ℓ and r_1 are the given length and radius of the projectile, x is the axial coordinate, and $r(x)$ is the projectile radius. The two terms in (2.1) correspond to Newtonian pressure drag and skin friction drag respectively. Omitting the constraint $r'\geqslant 0$, the shape shown in Figure 2.1 may possess smaller "drag" than any feasible shape for (2.1) above. However, this shape is physically nonoptimal since Newtonian theory is invalid wherever $r'(x)<0$. It can be shown that the physically optimal shape satisfies $r'\geqslant 0$ if base drag can be ignored. From a design viewpoint, base drag is significant, and a separate report [3] analyzes numerically the effect of base drag and projectile afterbodies. Nonetheless, even if base drag is included, the minimum drag problem must be decomposed into a forebody problem (like (2.1)) and an afterbody problem. Hence the results below apply to the forebody.

Although we constrain $r(0)=0$, a blunt nose shape can be achieved as the limit of a sequence of shapes satisfying $r(0)=0$. The blunt nose shape could also be treated by adding another term to the extremand in (2.1) corresponding to the nose radius and removing the constraint $r(0)=0$; however, the analysis is easier using the formulation (2.1).

Let D^* denote the infimum in (2.1). We say that r^* solves (2.1) if there exists a sequence of feasible shapes $\{r_k\}$ such that both $r_k(x)\to r^*(x)$ for almost every

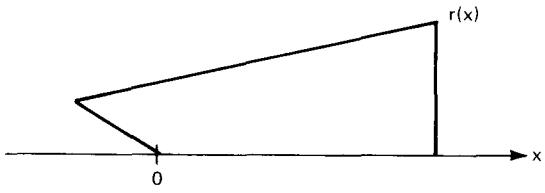

Fig. 2.1. A low drag shape for (2.1) omitting the constraint $r'\geqslant 0$.

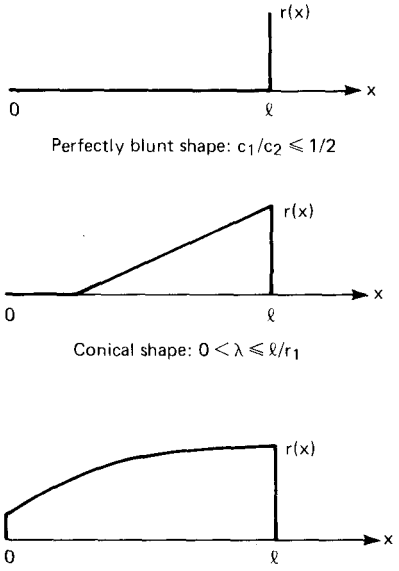

Fig. 2.2. Minimum drag shapes.

$x \in [0, \ell]$ and $D(r_k) \to D^*$. Defining the constant

$$\lambda = \sqrt{\left(\frac{2c_1}{c_2}\right)^{2/3} - 1}\ , \tag{2.2}$$

our principal theorem is the following:

Theorem 2.1. *For all values of* $c_1, c_2 \geqslant 0$, *there exists a unique solution to* (2.1). *If* $c_1/c_2 \leqslant 1/2$, $r^*(x) = 0$ *for* $x \in [0, \ell)$ *and* $r^*(\ell) = r_1$ (*perfectly blunt nose*). *If* $0 < \lambda \leqslant \ell/r_1$, *then* $r^*(x) = 0$ *for* $x \in [0, \ell - \lambda r_1]$ *and*

$$\frac{dr^*}{dx}(x) = \frac{1}{\lambda} \qquad \text{for } x \in [\ell - \lambda r_1, \ell] \tag{2.3}$$

(*conical shape*). *If* $\lambda > \ell/r_1$, *the nose of the optimal shape is partially blunt* (*see Figure* 2.2).

During the existence proof, an efficient algorithm is obtained for computing the partially blunt nose shape.

III. Change of Variables

Let us change variables to express (2.1) in terms of the independent variable $\rho = r^2$ and the dependent variable $g(\rho) = 1/r'$. In terms of g, the constraint

$r(\ell)=r_1$, becomes

$$\int_0^{r_1} g(r^2)\,dr=\ell. \tag{3.1}$$

Replacing r' by $1/g$ and $2r\,dr$ by $d\rho$ gives us the following equivalent formulation for (2.1):

$$\inf\left\{D(g)=\int_0^{r_1^2}\left[\frac{c_1}{1+g(\rho)^2}+c_2\sqrt{g(\rho)^2+1}\,\right]d\rho\right\} \tag{3.2}$$

subject to $g\geqslant 0$ and $\int_0^{r_1^2}\rho^{-1/2}g(\rho)\,d\rho=2\ell$.

IV. Perfectly Blunt and Conical Shapes

Define the function

$$h(g)=\frac{c_1}{1+g^2}+c_2\sqrt{1+g^2}\,, \tag{4.1}$$

the integrand of the extremand in (3.2). It is easy to see that the value of g minimizing $h(g)$ is given by: $g=0$ if $c_1/c_2<1/2$ and $g=\lambda$ if $c_1/c_2\geqslant 1/2$ (λ defined in (2.2)). First let us consider the case $c_1/c_2\geqslant 1/2$ and $\lambda\leqslant \ell/r_1$.

Since $h(g(\rho))\geqslant h(\lambda)$ for all $g(\cdot)$ and all ρ, we have $D^*\geqslant h(\lambda)r_1^2$. In fact, we show that $D^*=h(\lambda)r_1^2$. Define the following function:

$$g_n(\rho)=\begin{cases}\lambda & \text{for } \dfrac{r_1^2}{n^2}\leqslant\rho\leqslant r_1^2\\[2ex] \dfrac{\ell n}{r_1}+\lambda(1-n) & \text{for } 0\leqslant\rho\leqslant\dfrac{r_1^2}{n^2}\end{cases} \tag{4.2}$$

Since $\lambda\leqslant\ell/r_1$, both constraints in (3.2) are satisfied. Furthermore,

$$\left|\int_0^{r_1^2/n^2}h(g_n(\rho))\,d\rho\right|\leqslant\int_0^{r_1^2/n^2}\left[c_1+c_2\frac{\ell n}{r_1}\right]d\rho \qquad (n \text{ large})$$

$$=\left[c_1+c_2\frac{\ell n}{r_1}\right]\frac{r_1^2}{n^2}\to 0 \qquad (\text{as } n\to\infty). \tag{4.3}$$

On the other hand,

$$\int_{r_1^2/n^2}^{r_1^2} h(g_n(\rho))\,d\rho = h(\lambda)r_1^2\left[1-1/n^2\right]\to h(\lambda)r_1^2 \qquad (\text{as } n\to\infty). \tag{4.4}$$

Hence $D^* = h(\lambda)r_1^2$ as claimed. Since $g = 1/r'$, the shapes $r_n(x)$ corresponding to $g_n(\rho)$ converge to the conical shape described in Theorem 2.1. As $c_1/c_2\to 1/2$, $\lambda\to 0$ and r' becomes vertical at $x=\ell$. Hence the optimal shape becomes perfectly blunt.

The uniqueness proof is slightly technical and can be found in the Appendix.

V. Partially Blunt Nose

Usually $\lambda \gg \ell/r_1$ for caliber 5 projectiles and sea level conditions so g_n defined in (4.2) violates the constraint $g \geqslant 0$. We now apply Lagrange duality theory for convex control problems to the following equivalent formulation of (3.2):

$$(P) \qquad \inf\left\{ D(g) = \int_0^{r_1^2} h(g(\rho))\,d\rho \right\}$$

subject to $dw(\rho)/d\rho = \rho^{-1/2}g(\rho)$, $w(0)=0$, $w(r_1^2)=2\ell$. In control theory terminology, w and g are the state and the control respectively.

Since the function $h(g)$, plotted in Figure 5.1, is not convex, we must first convexify our problem. Let $\tilde{h}(g)$ be obtained by taking the convex hull of the epigraph set for h (see Figure 5.2), and let $(\tilde{P})$ be the same as (P) but with h replaced by $\tilde{h}$. Let us define

$$\tilde{D}(g) = \int_0^{r_1^2} \tilde{h}(g(\rho))\,d\rho, \tag{5.1}$$

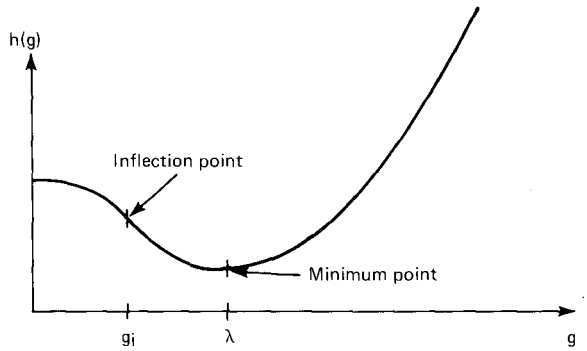

Fig. 5.1. The function h.

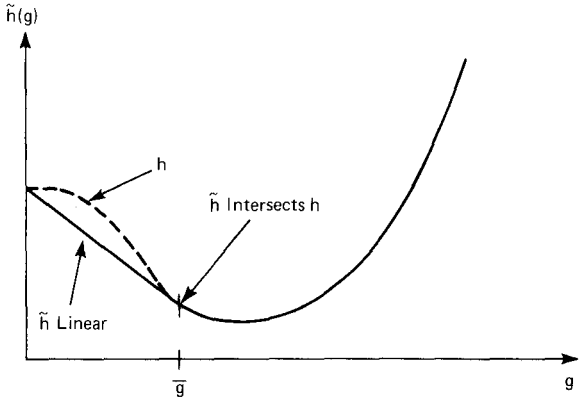

Fig. 5.2. The function $\tilde{h}$.

and let $\tilde{D}^*$ be the optimal value for $(\tilde{P})$. We show below that $\tilde{D}^* = D^*$; since $\tilde{h} \leqslant h$, we see that the optimal functions for (P) are also optimal for $(\tilde{P})$. On the other hand, by Lemma 5.1 below, there exists a unique optimum for $(\tilde{P})$ which is also optimal in (P) by Lemma 5.3.

First let us recall some results of Hager and Mitter. Define the Lagrangian

$$H(g,p,\rho) = \tilde{h}(g) + pg\rho^{-1/2}. \tag{5.2}$$

Since $(\tilde{P})$ is a convex control problem and the control coefficient $(\rho^{-1/2})$ in the differential equation is absolutely integrable, Theorems 1 and 3 and Lemma 1 in Hager-Mitter [2] imply that a feasible control $g^*(\rho)$ is optimal in $(\tilde{P})$ if and only if there exists a dual multiplier P such that

$$H(g^*(\rho),p,\rho) = \inf\{H(g,p,\rho) : g \geqslant 0\} \tag{5.3}$$

for almost every $\rho \in [0, r_1^2]$.

Lemma 5.1. *If $G(p,\rho)$ is the value of $g \geqslant 0$ that minimizes $H(g,p,\rho)$, then there exists a unique dual multiplier $p = p^*$ such that $G(p^*,\rho)$ satisfies the constraints for* (3.2). *(Hence $G(p^*,\rho)$ is the unique solution to $(\tilde{P})$).*

Remark 5.2. It can be shown that $G(p,\rho)$ is uniquely defined for all $\rho \neq \bar{\rho}$, where $\bar{\rho}$ (computed later) depends on c_1, c_2, and p. Furthermore, $G(p,\cdot)$ is infinitely differentiable for all $\rho \neq \bar{\rho}$ and $G(p,\cdot)$ jumps from $\bar{g}$ to zero at $\rho = \bar{\rho}$. Also we can prove that h'' only vanishes for $g = 0$ or g_i where $0 < g_i < \lambda$ (see Figure 5.1); hence $h''(g) > 0$ for $g > g_i$. Referring to Figure 5.2, we see that $\tilde{h} = h$ on $[\bar{g}, \infty)$ and $\bar{g} > g_i$; thus $\tilde{h}'' > 0$ on $[\bar{g}, \infty)$.

Proof of Lemma 5.1. We must prove the existence and uniqueness of p such that

$$\int_0^{r_1^2} \rho^{-1/2} G(p,\rho)\, d\rho = 2\ell. \tag{5.4}$$

To begin, (5.4) is simplified. Introduce the variable $z=\rho^{1/2}/p$ so that (5.2) assumes the form

$$H(g,z)=\tilde{h}(g)+g/z; \tag{5.5}$$

and let $G(z)$ minimize $H(g,z)$ over $g\geqslant 0$. Changing variables in (5.4) from ρ to z, we obtain

$$\int_0^{r_1/p} G(z)\,dz=\ell/p \qquad \text{or} \qquad \int_0^{\beta} G(z)\,dz=\left(\frac{\ell}{r_1}\right)\beta \tag{5.6}$$

where $\beta=r_1/p$.

We claim that (5.6) has no solution for $\beta<0$: Since $h'(g)<0$ for $0<g<\lambda$ and $h'(g)>0$ for $g>\lambda$, any solution to

$$\frac{d}{dg}H(g,z)=\tilde{h}'(g)+\frac{1}{z}=0 \tag{5.7}$$

satisfies $g>\lambda$ for $z<0$. Since $\lambda>\ell/r_1$, we have

$$\left|\int_0^{\beta} G(z)\,dz\right|>|\beta\lambda|>\left|\frac{\beta\ell}{r_1}\right|, \tag{5.8}$$

and the claim is established. □

In Figure 5.3, we plot $H(g,z)$ for various values of z. We see that there exists a critical value $\bar{z}$ such that

$$\begin{aligned} &h(0)=\text{minimum}\{H(g,z):g\geqslant 0\} \qquad \text{for all } 0<z<\bar{z}\\ &h(\bar{g})=\text{minimum}\{H(g,\bar{z}):g\geqslant 0\}. \end{aligned} \tag{5.9}$$

That is, $G(z)=0$ for all $0<z<\bar{z}$ and $G(\bar{z})=\bar{g}$. Hence (5.6) gives us the equation:

$$L(\beta)\equiv\int_{\bar{z}}^{\beta} G(z)\,dz-\frac{\ell}{r_1}\beta=0. \tag{5.10}$$

Since $\tilde{h}''>0$ on $[\bar{g},\infty)$, the solution $g=G(z)$ to the equation $\tilde{h}'(g)=-z^{-1}$ is an increasing function of $z\geqslant\bar{z}$. Furthermore, since $h'(\lambda)=0$, we see that $G(z)\to\lambda$ as $z\to\infty$. Combining these results, we have $L(\bar{z})<0$, $L'(\beta)=G(\beta)-\ell/r_1$ monotone increasing, and

$$\lim_{\beta\to\infty} L'(\beta)=\lambda-\frac{\ell}{r_1}>0. \tag{5.11}$$

Hence $L(\beta)=0$ has a unique, positive solution. (Note that $\beta=0$ is a trivial solution to (5.6), but $p=r_1/\beta$ is undefined for $\beta=0$).

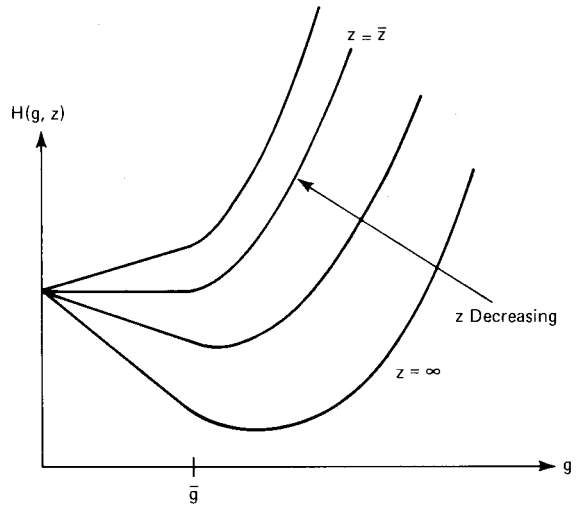

Fig. 5.3. $H(g,z)$ for various values of z.

Lemma 5.3. $D(G(p^*,\cdot))=\tilde{D}(G(p^*,\cdot))$.

Proof. As can be seen from Figure 5.3, $G(z)>\bar{g}$ for $z\geq\bar{z}$ and $G(z)=0$ for $z<\bar{z}$. But $h(g)=\tilde{h}(g)$ for $g=0$ or $g\geqslant\bar{g}$. Hence $h(G(z))=\tilde{h}(G(z))$ for $z\neq\bar{z}$ and the proof is complete since $G(p^*,\rho)=G(z=\rho^{1/2}/p^*)$. □

By Lemma 5.1, Lemma 5.3, and our earlier remarks, there exists a unique solution to (2.1) for $\lambda>\ell/r_1$.

Remark 5.4. The Pontryagin maximum principle is not immediately applicable to the problems (P) or $(\tilde{P})$ since the system dynamics are discontinuous. In the Lagrange duality paper [2], the usual continuity and smoothness assumptions were replaced by convexity assumptions; hence the duality theory could be applied directly to $(\tilde{P})$.

VI. Computation of the Optimal Dual Multiplier

To solve (5.10), $\bar{z}$ must be computed. Observe that $\bar{g}$, shown in Figures 5.2 and 5.3, has the following property: $h'(\bar{g})$ agrees with the slope of the secant connecting $(0,h(0))$ and $(\bar{g},h(\bar{g}))$. That is,

$$\frac{h(\bar{g})-h(0)}{\bar{g}}=h'(\bar{g}). \tag{6.1}$$

Defining $\alpha=\sqrt{1+\bar{g}^2}$ and omitting some algebra, (6.1) is equivalent to

$$(c_1+c_2)\alpha^4-c_2\alpha^3-3c_1\alpha^2+2c_1=0. \tag{6.2}$$

Knowing $\bar{g}$, we have $h'(\bar{g})+1/\bar{z}=0$ or $\bar{z}=-1/h'(\bar{g})$. Equation 6.2 has the trivial root $\alpha=1$ or $\bar{g}=0$. As $\bar{g}\to 0$, the left side of (6.1) defines the derivative at zero. Dividing out this trivial root, we obtain the equation:

$$m(\alpha)\equiv\left(1+\frac{c_2}{c_1}\right)\alpha^3+\alpha^2-2\alpha-2=0. \tag{6.3}$$

By the following relations, we see that $m(\alpha)$ has a unique positive zero: $m(0)<0$, $m''>0$ on $[0,\infty)$, and $m''(\alpha)\to\infty$ as $\alpha\to\infty$. For $0\leqslant c_2/c_1<2$ (nose not perfectly blunt), we have $m(1)\leqslant 0\leqslant m(\sqrt{2}\,)$. Hence the positive zero of $m(\alpha)$ lies on $[1,\sqrt{2}\,]$; since $m''>0$ for $\alpha>0$, it is well known that Newton's method converges quadratically to the positive zero from any non-negative starting condition. Omitting the algebra, we have:

$$\frac{1}{\bar{z}}=-h'(\bar{g})=\frac{\bar{g}}{\alpha^4}\left[2c_1-c_2\alpha^3\right]. \tag{6.4}$$

To determine p^* or equivalently the root $\beta^*=r_1/p^*$ to the equation $L(\beta)=0$, we numerically integrate $G(z)$ in (5.10) until $L(\beta)=0$. Since $G(z)$ is changing rapidly for z near $\bar{z}$ and slowly for $z\gg\bar{z}$, it is more efficient to integrate $G(z)$ using an exponentially growing step size rather than a uniform step size.

Note that $G(\bar{z})=\bar{g}$. As z increases incrementally in the integration process, $G(z)$ changes incrementally and hence $G(z)$ is easily computed using any equation solver for the equation $h'(g)=-1/z$. In particular, Newton's method was found to work well. After p^* has been determined, the corresponding optimal shape is found by integrating the equation:

$$\frac{dr(x)}{dx}=\frac{1}{G\left(\dfrac{r(x)}{p^*}\right)},\qquad r(x=0)=p^*\bar{z} \tag{6.5}$$

where $p^*\bar{z}$ is the radius of nose bluntness (recall that $z=\rho^{1/2}/p=r/p$ and $\bar{z}$ is the value of z where $G(z)=1/r'$ jumps from zero to a positive value).

Remark 6.1 (Behavior near nose). Observe that for $c_2/c_1=2$, the corresponding positive root α_+ of $m(\alpha)$ is 1; and as c_2/c_1 approaches zero, α_+ moves monotonically to $\sqrt{2}$. The slope of the nose, given by $r'(0)=(\alpha_+^2-1)^{-1/2}$, is plotted in Figure 6.1 as a function of c_2/c_1.

In Section 5 we saw that $G(z)$ was an increasing function of $z\geqslant\bar{z}$. Thus the optimal slope is a decreasing function of x. Potentially, the nose bluntness can be a large percentage of r_1. For example, if $c_2=0$, the radius of the nose satisfies $r(0)\geqslant r_1-\ell$ since the optimal slope is $\leqslant 1$. Hence the nose radius approaches r_1 as $\ell\to 0$. On the other hand, for caliber 5 projectiles, traveling at sea level conditions, the nose radius (computed numerically) is at most $(.01)r_1$.

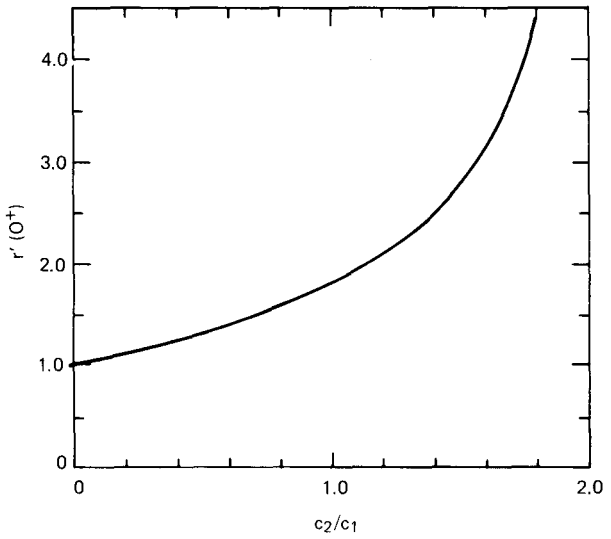

Fig. 6.1. Drag coefficients versus nose slope for partially blunt nose.

Appendix: Uniqueness of solution for perfectly blunt and conical geometry

For $c_1/c_2 > 1/2$ and $\lambda \leqslant \ell/r_1$, we now prove the unique optimality of the conical shape given in Theorem 2.1. Let $\{g_n\}$ be any minimizing sequence for (3.2), let $\epsilon > 0$ be a small constant, and define $N_n = \{\rho : |g_n(\rho) - \lambda| > \epsilon\}$. Since $D(g_n) \to D^*$ and $h(g_n(\rho)) \geqslant h(\lambda)$, we have measure $(N_n) \to 0$ as $n \to \infty$ and

$$\int_0^{r_1^2} \left[h(g_n(\rho)) - h(\lambda) \right] d\rho \to 0 \qquad \text{as } n \to \infty. \tag{A.1}$$

Let $k > 0$ be a large constant and define $M_n = \{\rho : |g_n(\rho) - \lambda| \geqslant k\} \subset N_n$. Observe the following relations:

$$\begin{aligned} D^* &= \lim_{n\to\infty} D(g_n) \geqslant \lim_{n\to\infty} \int_{[0,r_1^2]-M_n} h(g_n(\rho))\, d\rho \\ &\geqslant \lim_{n\to\infty} h(\lambda)\left[r_1^2 - \text{measure}(M_n) \right] = D^* \end{aligned} \tag{A.2}$$

Hence all the inequalities in (A.2) must be equalities. Combining (A.1) and (A.2) gives us:

$$\lim_{n\to\infty} \int_{M_n} h(g_n(\rho))\, d\rho = 0. \tag{A.3}$$

Since $\lim_{g\to\infty} |h(g) - c_2 g| = 0$, (A.3) implies that

$$\int_{M_n} g_n(\rho)\, d\rho < \epsilon \tag{A.4}$$

for all k, n sufficiently large.

Observe that the shape $x_n(\rho)$ corresponding to $g_n(\rho)$ is given by

$$x_n(\rho) = \ell - \int_{\rho}^{r_1^2} \tfrac{1}{2}\rho^{-1/2} g_n(\rho)\, d\rho. \tag{A.5}$$

Since measure $(N_n) \to 0$ as $n \to \infty$ and $\epsilon > 0$ was arbitrary, (A.4) and (A.5) imply that:

$$\lim_{n\to\infty} x_n(\rho) = \ell - \int_{\rho}^{r_1^2} \tfrac{1}{2}\rho^{-1/2}\lambda\, d\rho \qquad \text{for } r_1^2 \geqslant \rho > 0. \tag{A.6}$$

Since $\{g_n\}$ was an arbitrary minimizing sequence, the conical shape (A.6) is the unique optimum. The perfectly blunt geometry is treated similarly.

Acknowledgments

We wish to thank James Adams for computing Figure 6.1.

References

1. A. J. Eggers, Jr., Nonslender bodies of revolution having minimum pressure drag, *The Theory of Optimum Aerodynamic Shapes*, edited by A. Miele, Academic Press, New York, 1965.
2. W. W. Hager and S. K. Mitter, Lagrange duality theory for convex control problems, *SIAM J. Control and Optimization*, **14** (1976), 843–856.
3. W. W. Hager, F. G. Moore, and F. R. DeJarnette, *Optimal projectile shapes for minimum total drag*, Technical Report, Naval Surface Weapons Center, Silver Spring, Maryland.
4. H. Kennet, The effect of skin friction drag on optimum minimum-drag shapes in hypersonic flow, *J. Aerospace Sciences*, December 1962, 1486–1487.
5. A. Miele and D. G. Hull, Slender shapes of minimum total drag, *The Theory of Optimum Aerodynamic Shapes*, edited by A. Miele, Academic Press, New York, 1965.

Received July 18, 1977